Nonparametric preprocessing in system identification: a powerful tool

J. Schoukens, G. Vandersteen, K. Barbé, R. Pintelon

Vrije Universiteit Brussel, dep. ELEC, Pleinlaan 2, B1050 Brussels, Belgium
email: Johan.Schoukens@vub.ac.be

Abstract

In this paper we study the properties of existing nonparametric methods for estimating the plant and noise transfer functions of a linear dynamic system. The analysis is based on the recent insight that leakage errors in the frequency domain have a smooth nature that is completely similar to the initial transients in the time domain. This not only allows us to understand better the existing classic methods, but also opens the road to new better performing algorithms. The paper includes the output error setup, the errors-in-variables setup, and measurements under feedback conditions. Eventually, some of the methods are illustrated in the analysis of a vibrating metal beam.

1. Introduction

The aim of system identification is to provide a mathematical model for a dynamic system starting from measured inputs and outputs. Consider a linear dynamic discrete time system

$$y(t) = G_0(q)u_0(t) + H_0(q)e(t) = G_0(q)u_0(t) + v(t) \tag{1}$$

as shown in Figure 1 with with q^{-1} the backwards shift operator ($q^{-1}x(t) = x(t-1)$), and $e(t)$ white noise. In the standard identification problem, a linear dynamic model is identified for the system G_0, together with a model H_0 to describe the power spectrum $S_{VV} = |H_0|^2\sigma_e^2$ of the disturbing noise source $v(t)$. In the more general case, also

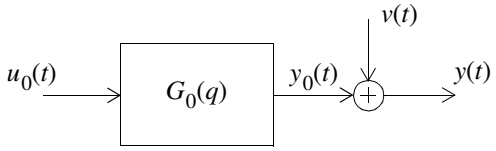

Fig. 1: Time domain representation of the simplified problem.

the input measurement is disturbed with noise. A lot of the standard identification literature is focussed on the parametric identification problem, aiming to deliver a parametric plant and noise model, respectively $G(q, \theta)$ and $H(q, \theta)$, with θ the model parameters [1],[2]. This work is dominantly done using a time domain formulation. In the more recent frequency domain formulation [3], the parametric noise model $H(q, \theta)$ is replaced by a nonparametric noise model, describing the noise $v(t)$ by its variance contribution $\sigma_v^2(\Omega_k)$ at the k^{th} frequency. Also the parametric plant model $G(q, \theta)$ can be replaced by its nonparametric frequency response function (FRF) representation $G(\Omega_k)$. This leads to a full nonparametric approach of the identification problem.

Even if parametric modeling is the final goal, the nonparametric modeling step can be a very interesting intermediate step, and this for many reasons. Nonparametric methods are non-iterative and require no user

interaction. As such they are an easy and fast possibility to get a first impression of the complexity of the modeling problem, providing the user with the FRF of the plant and the power spectrum of the disturbing noise. This allows the quality of the measurements to be verified at a very early stage of the experiment, giving the user the opportunity to improve the experiments if necessary. It is even possible to check for the presence of nonlinear distortions and to analyze their level and nature before starting a more demanding parametric identification process [4]. The FRF is also a very attractive tool for model validation/selection purposes.

Measuring the FRF of a linear dynamic system together with its variance is an old problem that is considered to be well solved and completely understood. The book [5] is a popular and classic reference work. In [5], a thorough theoretical analysis is made. The major disadvantage of the nonparametric approach is the presence of leakage problems that are intrinsically linked to the time-frequency domain transform. Even in the absence of disturbing noise, the FRF-measurements can be corrupted by these errors due to windowing effects: only a finite length record can be measured and processed. One possibility to get around these problems is to use periodic signals. By measuring an integer number of periods of the input and output signals, all leakage problems are avoided provided that the system transients decayed well below the noise level. But this is done at a cost of lost measurement time, because the transient information is not used. Moreover, in many applications the user wants to stick to random excitations, sometimes for technical reasons but often by tradition in a given application field. Random excitations are intrinsically linked to leakage problems.

Until the 80's, leakage errors on FRF-measurements were studied at the input and output signal level, without taking care for the linear system relation between the input and output [5], [7]. In a series of papers [8], [9], [10], [11], the importance of this relation was recognized: in FRF-measurements, the errors are due to unknown past inputs and missing future outputs. Both effects are highly structured, with smooth characteristics. It is this key observation that leads to a new analysis of the existing methods, and it is also a highway to new better performing methods to measure $G_0(\Omega_k)$ and $\left|H_0(\Omega_k)\right|^2$. An early attempt to use this insight for reducing the impact of leakage errors is due to [8], accounting explicitly for past inputs at a cost of an increased variance [12]. Alternatively, it is possible to compensate for the end effects, using an initial estimate of the impulse response which reduces also the leakage errors [11],[13]. The major disadvantage of these methods is their assumption that each processed (sub)record is longer than the dominating part of the impulse response. In this paper two other approaches will be followed to remove the leakage errors. In the first approach, 'non smooth excitations' called 'rough' signals, as defined more precisely later in this paper, will be used which will allow to separate the 'smooth' leakage part from the rest of the signal. The second approach relies on the use of periodic signals.

The paper is split in three parts. First we deal with the output error (OE) problem in which the noise is assumed to be present only at the output measurements. In the first part this problem is solved using random excitations, while the second part focuses on periodic excitations. In the third part we generalize the ideas to the errors-in-variables (EIV) problem for random and periodic excitations. In that case (mutually dependent) noise is allowed on all the signals, and it is even no longer necessary to classify the signals as an input or an output.

Spectral analysis methods, that model the power spectrum of a random signal, can be viewed as a special case within this framework where the system G_0 in (1) is zero. This will allow the classical windowing methods [14] to be considered in the same framework. It will turn out that windows basically differentiate the signals to remove

the smooth leakage errors, so that only the rough noisy part remains. But this is done at the cost of an additional interpolation error because measurements at neighbouring frequencies are combined. Different windows make a different balance between the leakage and the interpolation error.

Table 1 gives a schematic overview of the problems that will be discussed in this paper, as a function of the available measurements (see Fig. 4: r the reference signal, u_0, u the exact or disturbed measurement of the input, and y the disturbed measured output).

Table 1: Overview of the measurement problems that are studied in this paper

available signals and nature	results	experimental conditions
u_0, y rough signals	$G(\Omega_k)$, $S_{VV}(\Omega_k)$	OE and open loop
r, u, y rough signals	$G(\Omega_k)$, $\text{cov}(V_u(\Omega_k), V_y(\Omega_k))$	EIV and feedback
u, y periodic signals	$G(\Omega_k)$, $\text{cov}(V_u(\Omega_k), V_y(\Omega_k))$	EIV and feedback
y random signal	$S_{VV}(\Omega_k)$	

We will not focus on the technical details nor proofs, but we rather want to make the reader aware of the very powerful methods that are developed recently. At the same time, we present a general framework that allows the new and the old methods to be linked, and gives a generic understanding of many classic results. We first give a precise definition of the setup and the assumptions on the signals, the disturbing noise, and the system. Next we consider the output-error setup for rough signals (Part I) and periodic signals (Part II), followed by the errors-in-variables setup, including feedback, in Part III.

2. Problem statement and assumptions

2.1 Time-frequency transform

The results in this paper will be reported in the frequency domain, while the measurements are made in the time domain. Consider a sampled signal $x(t)$, measured at $t = 0, 1, \ldots, N-1$ (the sample period is normalized to 1 for simplicity). The discrete Fourier transform spectrum (DFT) is then defined to be:

$$X(k) = \frac{1}{\sqrt{N}} \sum_{t=0}^{N-1} x(t) e^{-j2\pi kt/N} . \tag{2}$$

Remark that $X(k) = O(N^0)$ (in mean square sense) for filtered white noise. 'Ordo' $O(x)$ stands for an arbitrary function with the property that $\lim_{x \to 0} |O(x)/x| < \infty$, for example $O(N^{-1/2})$ stands for a variable that decreases towards zero with a rate of $N^{-1/2}$. Under very weak conditions, it can be shown that $X(k)$ is asymptotically complex normally distributed, and $X(k)$, $X(l)$ are asymptotically independent. For example, $E(X(k)\overline{X(l)}) = O(N^{-1})$, $\forall k \neq l$ with $\overline{X}$ the complex conjugate of X [3].

2.2 Setup

Consider a discrete or continuous time linear dynamic SISO system G_0 that can be captured in a (nonlinear) stable feedback loop (see Figure 4). In some of the references that we use in this paper, it is assumed that the system is stable and causal, however, the proofs in those papers can be generalized to the unstable case by allowing for non-causal systems [15], [16].

Assumption 1 (*System)*: The system G_0 is a single input single output system that is allowed to be unstable if captured in a stabilizing feedback loop.

Depending upon the method that we will discuss, some assumptions will be imposed on the excitation signal $u_0(t)$. The basic idea that is used in many methods is that the errors have a smooth spectrum while this is not so for the excitation. The difference of the excitation spectrum, for example $U_0(k+1) - U_0(k)$ should not vanish to zero (the probability that it remains in the same order of magnitude as $|U_0(k)|$ should be 1), even if the record length $N \to \infty$. This is formalized in the definition of rough signals below. Due to its smooth spectrum, a transient response is not a rough signal, the 'normalized' difference of the transient spectrum $|T(k+1) - T(k)| / |T(k)| = O(N^{-1})$ (assuming that $|T(k)| \neq 0$).

Definition 1: *(Rough excitation of order n)*: The signal $u_0(t)$ with DFT-spectrum $U_0(k)$ is called rough of order n at frequency k if it meets the following requirement:

$$\left|\text{diff}^{(n)}(U_0(k))\right| = O_p(N^0), \tag{3}$$

with $\text{diff}^{(1)}(U_0(k)) = U_0(k+1) - U_0(k)$, and $O_p(x)$ an ordo(x) in probability.

This ensures that the DFT-spectrum $U_0(k)$ is not smooth so that it is not eliminated when a window is applied. A special case of such a signal is filtered white noise, but also deterministic signals can be rough. A swept sine excitation with period N that sweeps from $f_{\min}$ to $f_{\max}$ is not rough at all frequencies.

Assumption 2 (*Excitation signal)*: $u_0(t)$ is a signal with existing moments up to order 4, and has a DFT-spectrum $|U_0(k)|$ that is an $O(N^0)$.

Depending on the situation, additional assumptions on the excitation are imposed. These are collected in Assumption 3.

Assumption 3 (*Excitation signal, additional assumptions)*

a) *rough excitation of order n*: $u_0(t)$ is a rough signal of order n at frequency k.

b) $u_0(t)$ is a periodic signal with period $T_0 = NT_s$ with $T_s = 1/f_s$ the sample period, and N samples per period.

c) $u_0(t)$ has existing moments up to any order

Assumption a) is needed to be sure that the excitation signal and the corresponding output are rough enough in order to separate it from the smooth transient behaviour. Assumption b) will be imposed in the sections dealing with periodic excitations. Assumption c) is needed to get asymptotic normal distributed estimates for an increasing number of averages. Existing moments up to order 4 implies that the estimated 2nd order moments will converge for an increasing number of averages.

To study the noise properties of the methods, two situations are considered depending on whether the input is exactly known (OE) or not (EIV). The following assumption on the disturbing noise is made:

Assumption 4 (*Noise)*: the measurements are disturbed by filtered white noise $v(t) = h_0 * e(t)$ with $e(t)$ an i.i.d. random noise signal with existing moments up to order 4.

Depending on the situation, additional assumptions on the noise are imposed. These are collected in Assumption 5.

Assumption 5 *Noise: additional properties*

a) OE: the measured output is $y(t) = y_0(t) + v(t)$, the input is exactly known.

b) EIV: the measured input and output are disturbed by filtered i.i.d. noise: $u(t) = u_0(t) + v_u(t)$ and $y(t) = y_0(t) + v_y(t)$. The noise disturbances v_u, v_y can be mutually dependent.

c) the i.i.d. driving noise $e(t)$ has existing moments up of any order

3. Leakage revisited

In this section we study the relation between the DFT-spectra of two signals u_0, y_0 that are related by a linear dynamic system:

$$y_0(t) = g_0(t) * u_0(t). \tag{4}$$

The signals are sampled over a finite interval $t = 0, 1, \ldots, N-1$. Then it is shown [3], [17] that the following relation holds between the DFT-spectra at the generalized frequency $\Omega_k = j2\pi k f_s/N$ (continuous time systems) or $\Omega_k = e^{-j2\pi k f_s/N}$ (discrete time systems):

$$Y_0(k) = G_0(\Omega_k)U_0(k) + T_G(\Omega_k) \tag{5}$$

where $G_0(\Omega)$ is the system transfer function, and $T_G(\Omega)$ is a generalized transient term due to beginning and end effects induced by the finite measurement time. Under Assumption 2 it is an $O(N^{-1/2})$. Most important is to notice that not only G_0 but also the 'leakage' contribution T_G is a continuous function of the frequency. This shows that leakage is a highly structured effect with a smooth behaviour. This is the key observation that will not only be used to understand the existing methods but also to develop new methods. A detailed time-domain interpretation of these effects is given in [13].

Part I: The Output-Error setup for random excitations

In the first part we focus on the output-error problem, assuming that one of the signals, called the input $u_0(t)$, is known exactly, while the output is disturbed by noise $y(t) = y_0(t) + v(t)$. Without any loss of generality we assume for simplicity a single-input-single-output (SISO). In this part, three problems will be discussed: first we discuss how to measure the FRF starting from u_0, y. Next we discuss how to estimate the power spectrum S_{VV} from u_0, y knowing that there exists a linear relation between u_0, y_0. Finally it is discussed how a nonparametric spectral estimate S_{VV} can be obtained from $y(t) = v(t)$.

4. The classical FRF-measurement approach: windowing methods

4.1 Introduction

Assumptions: In this section we deal with the estimation of the FRF of the system G_0 assuming that the excitation-Assumption 3a (rough signal) is valid. First we consider the situation without disturbing noise distortions ($v(t) = 0$). Even in that case, leakage errors will be present. The estimated FRF $\hat{G}$ will be a random variable for random excitations like filtered white noise, and its mean value and bias can be calculated under these conditions. Under Assumption 3c it can be shown that $\hat{G}$ will be asymptotically normally distributed.

Method: The most simple idea to measure the FRF is a division of the output and input spectrum:

$$\hat{G}(\Omega_k) = \frac{Y_0(k)}{U_0(k)} = G_0(\Omega_k) + \frac{T_G(\Omega_k)}{U_0(k)}. \tag{6}$$

This estimate is also called the empirical transfer function estimate ETFE [1]. Equation (6) reveals the basic problem with this direct approach: the presence of the leakage term $T_G(\Omega_k)$ that is significantly amplified at those frequencies where $U_0(k)$ is very small. Since $U_0(k)$ is a zero mean complex normally distributed random variable for random excitations, it can become arbitrary small at some frequencies, and the error $T_G(\Omega_k)/U_0(k)$ can become arbitrary large leading to a non-existing variance [18]. To avoid this, an averaging procedure is used so that the denominator comes closer to its expected value (that is assumed to be different from zero) before the division is made. For that reason the input-output records are split in M sub-records, ${u_0}^{[m]}$, ${y_0}^{[m]}$ $m = 1, \ldots, M$, with length N each, and the averaged estimate is:

$$\hat{G}_R(\Omega_k) = \frac{\sum_{m=1}^{M} Y_0^{[m]}(k)\,\overline{U_0}^{[m]}(k)}{\sum_{m=1}^{M} \left|{U_0}^{[m]}(k)\right|^2} = \frac{\hat{S}_{YU}(k)}{\hat{S}_{UU}(k)}. \tag{7}$$

with

$$\hat{S}_{YU}(k) = \frac{1}{M}\sum_{m=1}^{M} Y_0^{[m]}(k)\,\overline{U_0}^{[m]}(k) \qquad \hat{S}_{UU}(k) = \frac{1}{M}\sum_{m=1}^{M} \left|{U_0}^{[m]}(k)\right|^2 \tag{8}$$

the sample estimates of the cross- and auto-spectrum. The most important result is the removal of the large spikes of the error term because $\lim_{M\to\infty} \hat{G}(\Omega_k) = S_{Y_0U_0}(k)/S_{U_0U_0}(k)$ so that in the limit $U_0(k)$ in (6) is replaced by $S_{U_0U_0}(k)$. The stochastic properties are well known [5], [3], [18].

4.2 Effect of a window on the DFT-spectrum

A second classical step to further reduce the impact of the leakage error is to use a window. The measured time signals are multiplied with a window $w(t)$ to reduce the edge effects. The original DFT-spectra are replaced by the windowed DFT-spectra $X_W = \mathrm{DFT}(x(t)w(t))$. In the spectral domain, the windowed spectrum is retrieved by making the convolution between the DFT-spectrum $X(k)$ and the DFT-spectrum $W(k)$ of the window:

$$X_W(k) = \sum_{r=-L}^{L} X(k-r)\,W(r), \tag{9}$$

where L is the spectral width of the window.

4.3 The Hanning-window

The most popular window is the Hanning-window with $w(t) = 0.5 - 0.5\cos(2\pi t/N)$, or $W([-1, 0, 1]) = [-0.5, 1, -0.5]$. The relation between the DFT-spectrum and the 'Hanning-spectrum' is:

$$X_{\mathrm{Hann}}(k) = 0.25[2X(k) - X(k-1) - X(k+1)]. \tag{10}$$

Observe that this is nothing than a double difference of the original spectrum. In (5), the term $G_0(k)U_0(k)$ is not a smooth function of k for random excitations, but $T_G(k)$ is. Using a Taylor expansion, it can be rewritten as

$$T_G(k \pm 1) \;=\; T_G(k) \pm \frac{t_1(k)}{N} + \frac{t_2(k)}{N^2} + O(N^{-1/2})O(N^{-3}) \tag{11}$$

with t_1, t_2 an $O(N^{-1/2})$ because also T_G is an $O(N^{-1/2})$, and the frequency step is an $O(N^{-1})$. Hence differencing the output spectrum $Y(k)$ twice as is done with a Hanning window reduces the leakage term with a factor $O(N^2)$. This can be generalized to other windows by interpreting the time window $w(t) \;=\; \mathrm{DFT}^{-1}\{W(k)\}$ as the amplitude characteristic of the difference filter that is used to suppress the smooth terms in the frequency domain in (5). So $w(t)$ can be seen as the transfer function of the difference filter and windows with $w(0) \;=\; 0$ (transfer function at DC = 0) will remove a constant value in the frequency domain. Hence such windows act as a difference of a given order and they reduce the leakage term with at least an $O(N^{-1})$.

However, in relation (5) a new interpolation error is created because also $G_0(\Omega_k)$ is varying with the frequency, and in the differencing process the frequencies $[k-1, k, k+1]$ are combined. This interpolation error is an $O(N^{-1})$ because G_0 is an $O(N^0)$ that is a smooth function of the frequency. So by applying a Hanning-window in the spectral analysis, the leakage error is reduced from $O(N^{-1/2})$ to $O(N^{-5/2})$, but a new interpolation error of $O(N^{-1})$ will mostly dominate the results.

The behaviour of the Hanning-window and alternatives are studied in detail in [19], [20]. In this paper the bias and variance contributions to the FRF-measurement of these errors is also quantified (See Table 2).

4.4 Alternative windows: the Diff-window

From the previous analysis, it follows that a Hanning-window replaces the dominating leakage error by a dominating interpolation error using a double difference. A similar effect can also be obtained by making only a single difference. The major advantage is that only two spectral lines are combined instead of three, so that the interpolation error will be smaller, while the leakage term T_G will still be reduced to $O(N^{-1/2})O(N^{-1})$. This leads to the definition of the Diff-window:

$$X_{\mathrm{DIFF}}(k) \;=\; X(k+1) - X(k)\,. \tag{12}$$

With the DIFF-window, the FRF is calculated at the middle frequency $\Omega_{k+1/2} \;=\; 2\pi\left(k + \frac{1}{2}\right)\frac{f_s}{N}$. An alternative to avoid this frequency shift is to use the half-sine-window [19]. It is shown that this window has the same properties as the DIFF-window, but it avoids the frequency shift.

An overview of the bias and variance errors on the FRF-measurements using the rectangular (do-nothing-window), DIFF, and Hanning-window is given in Table 2. It is not possible to make a generally valid best choice between the Diff- and the Hanning-window, the result will depend on the situation. In those frequency bands where the interpolation error dominates (typically around the resonance frequencies), the Diff window will perform better. However, around transmission zeros, the leakage errors often dominate and in that case the Hanning window will be the best choice.

4.5 Impact of disturbing noise

The impact of disturbing noise is studied under the Assumption 5a (OE-framework). In addition, if Assumption 5c holds, the estimates will be asymptotically normally distributed estimates, otherwise only the convergence of the variance estimates is guaranteed.

The induced variance is:

$$\sigma_G^2(k) = \frac{\sigma_V^2(k)}{ME\{\left|U_0(k)\right|^2\}}. \tag{13}$$

This expression is the same for the three window-methods (rectangular, DIFF, Hanning). Moreover, for filtered white noise excitations, the asymptotic ($M \to \infty$) normalized value of $M\sigma_G^2(k)$ is not affected by the choice of the window in those frequency bands where the noise filter has no weakly damped pole or transmission zero. At a sharp resonance peak of the noise filter the Diff window will be better than the Hanning window (smaller interpolation error). At a transmission zero of the noise filter, the Hanning window will be the best choice (leakage term dominates).

The variance that is induced by the leakage and the noise can be further reduced by using overlapping sub-records. This idea was initially used in spectral estimation [21], but it is later also applied to FRF estimation without much further analysis, until recently a number of studies were published [19], [23] that studied the behaviour on FRF-measurements in more detail. Traditionally an overlap of 50% is used, but a recent detailed analysis [19] has shown that optimal results are obtained for a 2/3th overlap or even higher, resulting in an additional 30% reduction of the systematic and stochastic errors that are induced by leakage. Overall, using a 2/3th overlap, a reduction in leakage induced variance with a factor of 3 can be obtained (except at the zero and folding frequencies) compared to the non-overlapping situation. The variance due to the measurement noise is reduced with about a factor two. These numbers depend slightly on the window type.

4.6 Conclusion

The insight into the smooth nature of leakage errors gives a simple tool to understand better the behaviour of different windows. Moreover, this insight has been used to propose a new window, the DIFF-window. In the next Section, it will be used to develop a new method.

5. An improved FRF-estimation method: the local polynomial method

In this section we propose a very powerful nonparametric method to estimate the FRF using local polynomial models. These allow to make optimal use of the smooth behaviour of G_0 and T_G to eliminate the leakage and interpolation errors at the same time. This results in superior properties compared with the classical windowing approaches. A detailed description of the method for the MIMO-case is given in [15], here we restrict the scope again to the SISO-situation. It should be emphasized that the local polynomial method is always applied to the DFT-spectrum calculated from the full data record without splitting it in sub-records.

5.1 General relation between the DFT-spectra

In this section we start from the full expression $y(t) = G_0(q)u_0(t) + H_0(q)e(t)$, and consider again the equivalent relation for the DFT-spectra, but this time applied to the plant and the noise term:

$$\begin{aligned} Y(k) &= G_0(\Omega_k)U_0(k) + T_G(\Omega_k) + H_0(\Omega_k)E(k) + T_H(\Omega_k) \\ &= G_0(\Omega_k)U_0(k) + T(\Omega_k) + V_0(k) \end{aligned} \tag{14}$$

where the generalized transient term $T(\Omega_k) = T_G(\Omega_k) + T_H(\Omega_k)$ accounts for the leakage of the plant and noise dynamics. It is still an $O(N^{-1/2})$. The remaining noise term is $V_0(k) = H_0(\Omega_k)E(k)$, with $E(k)$ circular complex white noise [3]. The terms $G_0(\Omega_k)U_0(k)$ and $V_0(k)$ are an $O(N^0)$.

5.2 Linear-least-squares estimate

Making use of the smoothness of G_0 and T, the following Taylor series representation holds for the frequency lines $k + r$, with $r = 0, \pm 1, \ldots, \pm n$.

$$\begin{aligned} G_0(\Omega_{k+r}) &= G_0(\Omega_k) + \sum_{s=1}^{R} g_s(k) r^s + O((r/(NM))^{(R+1)}) \\ T(\Omega_{k+r}) &= T(\Omega_k) + \sum_{s=1}^{R} t_s(k) r^s + N^{-1/2} O((r/(NM))^{(R+1)}) \end{aligned} . \tag{15}$$

Putting all parameters $G_0(\Omega_k), T(\Omega_k)$ and the parameters of the Taylor series g_p, t_p, $p = 1, \ldots, R$ in a column vector θ, and their respective coefficients in a row vector $K(k, r)$ allows (14) to be rewritten (neglecting the remainders) as:

$$Y(k + r) = K(k, r)\theta + V_0(k), \tag{16}$$

Collecting (16) for $r = -n, -n + 1, \ldots, 0, \ldots, n$ finally gives

$$Y_n = K_n\theta + V_n, \tag{17}$$

with Y_n, V_n, K_n the values of $Y(k + r), V_0(k + r), K(k, r)$, stacked on top of each other. Observe that the matrix K depends upon U_0. Solving this equation in least square sense eventually provides the polynomial least squares estimate for $\hat{G}_{\text{poly}}(\Omega_k)$. In order to get a full rank matrix K_n, enough spectral lines should be combined: $n \geq R + 1$. The smallest interpolation error is obtained for $n = R + 1$.

5.3 Stochastic properties of $\hat{G}_{\text{poly}}(\Omega_k)$

A detailed analysis of the stochastic properties is made in [15] showing the following results.

Bias

$$E\left\{\hat{G}_{\text{poly}}(\Omega_k)\right\} = G_0(\Omega_k) + e_{\text{leak}G} + e_{\text{int}G}, \tag{18}$$

with $e_{\text{leak}G} = O((n/(NM))^{(R+2)})$ the remaining leakage error, and $e_{\text{int}G} = G_0^{(R+1)}(\Omega_k)O((n/(NM))^{(R+1)})$ the error due to the polynomial interpolation over the $2n + 1$ frequencies.

Variance

The variance in the absence of disturbing noise ($v = 0$) is given by:

$$\text{var}(\hat{G}_{\text{poly}}(\Omega_k)) = \left|G_0^{(R+1)}(\Omega_k)\right|^2 O((n/(NM))^{2(R+1)}) + O((n/(NM))^{(2R+3)}) = \sigma^2_{\text{int}G} + \sigma^2_{\text{leak}G}, \tag{19}$$

with $\sigma^2_{\text{int}G}, \sigma^2_{\text{leak}G}$ respectively the variance of the interpolation and leakage error.

5.4 Discussion

The polynomial method is a very powerful method. The optimal choice for R is case dependent. The interpolation error depends on n that grows proportionally to R. So R should be chosen not too high. However, the leakage error drops with R so that its value should be high enough. A good compromise is $R = 2$. A comparison with the errors of the window methods for the noiseless case is given in Table 2. This table shows clearly the superior properties of the polynomial method. The price to be paid for these better properties is a more involved calculation. However, due to these better properties it is possible to reduce the measurement time because shorter data records can be used. While computation power is becoming cheaper over the years, measurement time remains expensive in many applications which favours the use of the polynomial method in the future. It can also be remarked that

Table 2: Comparison of the errors on $\hat{G}_{\text{window}}$ for a rectangular, Hanning, and Diff window for the noiseless case ($v(t) = 0$) and M sub-records of length N.

method/assumption	leakage error	interpolation error	bias ($M \to \infty$)	variance
$w_{\text{Rect}}(k) = 1$ (Assumption 2a,)	$O(N^{-1/2})$	0	$O(N^{-1})$	$O(M^{-1}N^{-1})$
$w_{\text{Hann}}(k) = 0.5\left(1 - \cos k\frac{2\pi}{N}\right)$ (Assumption 2a, $n = 2$)	$O(N^{-5/2})$	$O(N^{-1})$	$O(N^{-2})$	$O(M^{-1}N^{-2})$
$w_{\text{Diff}}(k) = 1 - e^{j2\pi k/N}$ or $w_{\text{half-sine}}(k) = \sin \pi k/N$ (Assumption 2a, $n = 1$)	$O(N^{-3/2})$	$O(N^{-1})$	$O(N^{-2})$	$O(M^{-1}N^{-2})$
Polynomial ($R = 2$) (Assumption 2)	$O((NM)^{-7/2})$	$O((NM)^{-3})$	$O((NM)^{-3})$	$O((NM)^{-6})$

these methods do not only remove leakage effects, also other smooth errors like drift [22] will be suppressed.

6. Spectral analysis of the disturbing noise on the output of a linear dynamic system

Besides obtaining a good estimate for the FRF, it is also important to estimate the power spectrum of the noise. In a nonparametric modelling approach, the estimated variance $\hat{\sigma}^2_V(k)$ can be used. Also these estimates suffer from the leakage. As can be seen from (14), the DFT-spectrum $V(k) = H_0(\Omega_k)E(k) + T_H(\Omega_k) = V_0(k) + T_H(\Omega_k)$ is also disturbed by the leakage term $T_H(\Omega_k)$. What is really needed is information on the leakage free contribution:

$$\sigma^2_{V_0}(k) = E\{\left|V_0(k)\right|^2\} = \left|H_0(\Omega_k)\right|^2. \tag{20}$$

It is clear that this problem is very similar to the estimation of the FRF, but this time we focus on the disturbing noise term. We first consider again the classical spectral approach, based on the estimated auto- and cross-correlation spectrum in combination with the possible choices for the window. Next we estimate $\sigma^2_{V_0}(k)$ from the least square residuals of the polynomial method. The analysis of the stochastic properties will be done starting from (14).

6.1 Window methods

The start of the window methods is the observation that

$$\sigma_{V_0}^2 = S_{YY} - |S_{YU}|^2 / S_{UU}. \tag{21}$$

However, for finite length measurements, the sample estimates (8) for the cross- and auto-spectra are disturbed with leakage. For that reason, the use of the windowed spectra is also popular in this case. In classical implementations, it is indirectly measured by the coherence [5], [24]. In order to get an absolute estimate of the noise variance, normalized windows should be used, requiring a scaling of the window $w(t)$ of length N as $\sqrt{\alpha_W} w(t)$ with:

$$\alpha_W = \frac{N}{\sum_{t=0}^{N-1} w^2(t)}. \tag{22}$$

For a rectangular window $\alpha_W = 1$, for a Diff window $\alpha_W = 1/2$, for a half-sine window it is $\alpha_W = 2$, and for a Hanning window it is $\alpha_W = 8/3$. The analysis of the properties of the estimates for the different windows is very similar to that in the previous section. The results are summarized in Table3.

6.2 Polynomial method

Also the polynomial method can be applied to solve the spectral estimation of the disturbing noise problem. The method [15], [25] starts from the residuals of the least squares solution of (17):

$$\hat{V}_{0n} = Y_n - K_n \hat{\theta} = Y_n P_n, \tag{23}$$

with $P_n = I_{2n+1} - K_n (K_n^H K_n)^{-1} K_n^H$ an idempotent projection matrix, and $\hat{V}_{0n} = V_{0n} P_n$. The estimated variance is:

$$\hat{\sigma}_{\bar{V}_0}^2(k) = \frac{1}{q} \sum_{r=-n}^{n+r} |\hat{V}_{0n}(k+r)|^2, \tag{24}$$

with $q = 2(n-R) - 1$. For the minimal choice $n = R + 1$, we get that $q = 1$.

Instead of making a direct implementation of (23), it is better to use a numerical stable implementation $P_n = U^{\perp}(U^{\perp})^H$ as explained in [15] based on an SVD of $K_n = U \Sigma V^H$, and $U^{\perp}$ the orthogonal complement of U. The major advantage is that this expression is also valid in the absence of an excitation signal. This observation will also be used in Section 7 for the spectral estimation of random signals.

The error analysis in Table 3 shows a very high rejection of leakage errors. Because the method assumes that the

Table 3: Comparison of the errors on $E\{\hat{\sigma}^2_{V_0}(k)\}$ for a rectangular, Hanning, and Diff window for the noiseless case ($v(t) = 0$) and M sub-records with length N

method/assumption	leakage error	interpolation error
$w_{\text{Rect}}(k) = 1$ (Assumption 2)	$O(N^{-1})$	0
$w_{\text{Hann}}(k) = 0.5\left(1 - \cos k\frac{2\pi}{N}\right)$ (Assumption 2a, $n = 2$)	$S^{(1)}_{V_0}(k)O(N^{-3}) + O(N^{-5})$	$S^{(2)}_{V_0}(k)O(N^{-2}) + O(N^{-2})G^{(1)}_0(\Omega_k)^2$
$w_{\text{Diff}}(k) = 1 - e^{j2\pi k/N}$ or $w_{\text{half-sine}}(k) = \sin\pi k/N$ (Assumption 2a, $n = 1$)	$S^{(1)}_{V_0}(k)O(N^{-2}) + O(N^{-3})$	$S^{(2)}_{V_0}(k)O(N^{-2}) + O(N^{-2})G^{(1)}_0(\Omega_k)^2$
Polynomial ($R = 2$) (Assumption 2)	$S^{(1)}_{V_0}(k)O(\left(\frac{n}{MN}\right)^4) + O(\left(\frac{n}{MN}\right)^7)$	$S^{(1)}_{V_0}(k)O(\frac{n}{MN}) + O(\left(\frac{n}{MN}\right)^6)G^{(3)}_0(\Omega_k)^2$

noise variance is constant over all $2n + 1$ frequencies, an interpolation of $S^{(1)}_{V_0}(k)O(\left(\frac{n}{MN}\right))$ is introduced, with MN the total length of the data record. However, in most cases this will not be the dominating term, because the interpolation error is localized in frequency: as shown in Fig. 2, it does not carry over errors from one frequency band (for example with a high noise level) to another band (for example with a low noise level) which is the case for the leakage errors. That effect makes leakage errors a much more disturbing problem in noise analysis than the

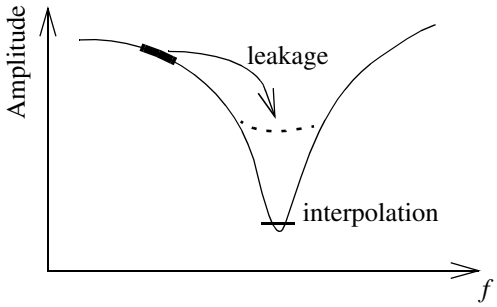

Fig. 2: Illustration of the different nature of the leakage error (transfer from one frequency band to the other) and the local behavior of the interpolation error.

interpolation error. For example, the interpolation error will be very small at transmission zeros of the noise model ($S^{(1)}_{V_0}(k) \to 0$), the leakage error will there be the dominant error. For slowly varying spectra (e.g. white noise) it will be small because $S^{(1)}_{V_0}$ goes to zero.

6.3 Conclusion

All the conclusions that were made in Section 5.4 apply also to the spectral estimation of the disturbing noise term.

7. Special case: spectral analysis of random signals

In Section 6.2 it was indicated that the expression is also valid in the absence of an excitation signal ($U(k) = 0$), starting from the relation

$$V(k) = H_0(\Omega_k)E(k) + T_H(\Omega_k)\,. \tag{25}$$

Under these conditions the method will estimate the $V_0(k) = H_0(\Omega_k)E(k)$ contribution while it eliminates the leakage contribution $T_H(\Omega_k)$ in the noise power spectrum estimate. This transforms the polynomial method into a powerful nonparametric spectral analysis method. Also the window methods can be applied to spectral analysis (periodogram). The same error analysis techniques can be applied as before on the basis of the relation (25). The results are given in Table 4. As mentioned before, it is the leakage error that is most important in practical use

Table 4: Comparison of the errors on $E\{\hat{\sigma}^2_{V_0}(k)\}$ for a rectangular, Hanning, and Diff window for the noiseless case ($v(t) = 0$) for M sub-records of length N

method	leakage error	interpolation error
$w_{\text{Rect}}(k) = 1$	$O(N^{-1})$	0
$w_{\text{Hann}}(k) = 0.5\left(1 - \cos k\frac{2\pi}{N}\right)$	$S^{(1)}_{V_0}(k)O(N^{-3}) + O(N^{-5})$	$S^{(2)}_{V_0}(k)O(N^{-2})$
$w_{\text{Diff}}(k) = 1 - e^{j2\pi k/N}$ or $w_{\text{half-sine}}(k) = \sin\pi k/N$	$S^{(1)}_{V_0}(k)O(N^{-2}) + O(N^{-3})$	$S^{(2)}_{V_0}(k)O(N^{-2})$
Polynomial ($R = 2$)	$S^{(1)}_{V_0}(k)O(\left(\frac{n}{MN}\right)^4) + O(\left(\frac{n}{MN}\right)^7)$	$S^{(1)}_{V_0}(k)O(\left(\frac{n}{MN}\right))$

because it mixes the power from different frequency bands. This is not so for the interpolation error. From all these results it is obvious that the polynomial method has superior characteristics in most applications.

Remark: The reader should be aware that besides the errors that are discussed in this section, every power spectral estimator has an intrinsic variance that is proportional to the squared power. The reader is referred to Section 11 for a further discussion on this topic.

Part II: Use of Periodic Excitations

In the second part of this paper, we analyse how to measure the FRF of a linear dynamic system, making explicit use of the assumption that the excitation signals are periodic (Assumption 2c). Although this imposes a significant experimental constraint on the freedom of the user, it also offers significant advantages. The measurement of the FRF becomes extremely simple, and also the noise analysis can be easily made if the measurements are made under steady state conditions. In some applications it might be too expensive to wait for the transients to become sufficiently small. In that case the user can combine the methods of Part II with those of Part I to eliminate the errors induced by the transient effects, while maintaining the advantages of periodic excitation.

8. Design of periodic excitations

Imposing the periodicity assumption of the excitation signal creates also a new experimental challenge. Using an arbitrary waveform generator that periodically generates a signal that is stored in its memory makes it possible to create arbitrary periodic signals. This leaves a lot of freedom to the user to choose these signals, opening the field

for optimal excitation signal design [3]. Since every periodic signal can be written as an infinite sum of sines, multisine signals can be selected as the general representation of periodic signals with a band limited spectrum:

$$u_0(t) = \frac{1}{\sqrt{N-2}} \sum_{\substack{k=-N/2+1 \\ k \neq 0}}^{N/2-1} U_k e^{j\left(2\pi k \frac{t}{N} + \varphi_k\right)} = \frac{1}{\sqrt{N-2}} \sum_{k=1}^{N/2-1} 2U_k \cos\left(2\pi k \frac{t}{N} + \varphi_k\right). \tag{26}$$

The design of the signal reduces to the selection of U_k and φ_k. Both the amplitude and phase can be either randomly or deterministically selected. This also allows signals with a mixed nature to be created. For example, using a deterministic amplitude spectrum U_k and a random phase uniformly distributed in $[0, 2\pi[$ creates signals with a Gaussian amplitude distribution. The major advantage is that even after a single realization the observed amplitude spectrum equals the desired one. Alternatively, it is possible to design the phase φ_k such that for a user defined U_k, a compact signal is obtained with a minimal crest factor [26]. This allows for a maximal power injection for a given amplitude constraint. Of course the users freedom is not restricted to these two examples.

9. The importance of synchronization

In order to exploit the advantages of periodic excitations, it is not enough to generate these signals, it will also be required to process an integer number of periods in order to avoid leakage of the plant dynamics in the DFT-spectra. A first possibility to realize this is to use a common clock for both the generator and the data acquisition so that the generator and acquisition are perfectly synchronized. This synchronization condition is very strict and should be carefully checked, the leakage error of $X(k)$ on line $k \pm 1$ is given by $k\varepsilon_{f_{\text{clock}}}|X(k)|$, with $\varepsilon_{f_{\text{clock}}}$ the relative error on the clock frequencies. A relative error of 10^{-4} between the clock frequencies of generator and data-acquisition creates already a relative leakage error of 10% at spectral line $k = 100$.

If the measurement equipment is not well synchronized, it is also possible to correct for it in a post processing step, but this is out of the scope of this paper [27]. This methods replaces the very hard synchronization requirement by a much weaker one: it is enough that the clock frequencies are stable in time.

10. Measuring the FRF using sample mean and sample variance

In this section we assume that the plant transient decayed to zero, so that the steady state conditions are reached. In that case the estimate of the frequency response function is calculated from the sample means of the input and output DFT-spectra, obtained from M measured periods:

$$\hat{G}_{\text{per}}(\Omega_k) = \frac{\hat{Y}(k)}{\hat{U}(k)} = \frac{\frac{1}{M}\sum_{i=1}^{M} Y^{[i]}(k)}{\frac{1}{M}\sum_{i=1}^{M} U^{[i]}(k)}, \tag{27}$$

where the index $^{[i]}$ indicates the DFT-spectrum from the i^{th} sub-record that corresponds to the i^{th} measured period. The DFT's are calculated using the rectangular window since no plant leakage is present. The reader should be aware that the transients of the noise filter are not optimal reduced this way. More advanced processing techniques using data blocks of two periods in combination with a Hanning window, can also reduce these effects, but this is out of the scope of this paper [30]. Of course it is also possible to estimate at the same time the sample-variance:

$$\hat{\sigma}^2_{\hat{Y}}(k) = \frac{1}{M-1}\sum_{l=1}^{M} \left|Y^{[l]}(k) - \hat{Y}(k)\right|^2 \tag{28}$$

The variance on the FRF is then estimated as:

$$\sigma^2_{\hat{G}_{\text{per}}}(\Omega_k) \approx \frac{\left|\hat{G}_{\text{per}}(\Omega_k)\right|^2}{M} \frac{\hat{\sigma}^2_{\hat{Y}}(k)}{\left|\hat{Y}(k)\right|^2} = \frac{\hat{\sigma}^2_{\hat{Y}}(k)}{M\left|\hat{U}(k)\right|^2}. \tag{29}$$

The major advantage of this approach is that it can be calculated very efficiently using FFT's. Moreover, as will be seen in Part III, the procedure can also be applied to the full errors-in-variables setup, including measurements under (non)linear feedback conditions.

11. Improved estimation of the noise variance using overlapping windows

By analysing sub-records that contain an integer number of periods, it is possible to separate the true signal $y_0(t)$ and the noise $v(t)$, because y_0 does not vary from one period to the other, while the disturbing noise $v(t)$ does. This opens the possibility for an analysis of disturbing noise on periodic signals without requiring a linear relation $y_0 = g_0 * u_0$ between a known input and measured output signal. In Section 6 this linear relation was required to remove the true signal y_0 from the noisy measurement $y = y_0 + v$ in order to get access to $v(t)$.

The sample variance estimate (28) can be improved by using overlapping windows [5], [21], [23]. The reader should be aware that this does not reduce $\sigma_{\hat{G}_{\text{per}}}$, only the estimates of the variance become more reliable. As mentioned before, using overlapping windows is a popular and well known method, that slightly modifies the procedure explained before. Instead of selecting non-overlapping sub-records, a user defined overlap between successive segments is now allowed. The advantage is that more sub-records are averaged, resulting in a decreasing variance of the variance estimate. This strategy can be combined with the different choices for the window. The major disadvantage of the classical Welch method is that this decrease is not monotonous as a function of the fraction of the overlap. When the overlapping becomes large, the variance on the variance estimates starts to increase again. Recent results [28] have shown that this can be avoided by using a circular overlap as shown in Fig 3. On top of that an extra reduction in variance with respect to the Welch method is obtained, at a cost of a slight

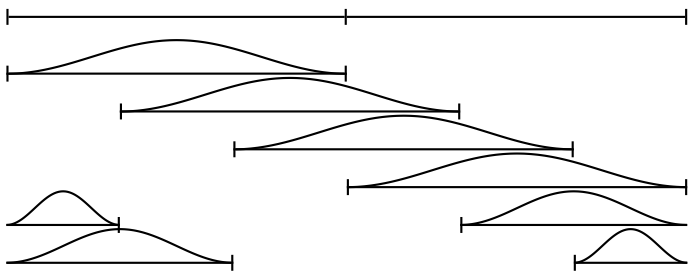

Fig. 3: Illustration of circular overlap (66.6%) using a Hanning window for a measurement with 2 periods $M = 2$. Notice that segments that cross the 'border' are covered by a combination of two Hanning windows, such that the windows are zero at the border.

increase of the bias errors. The reduction in variance is significant for a small number M of measured periods. In this paper, we just report the major results of [28] in Table 2. The normalized final variance $M\sigma^2_{S_{V_0}}(k)/S_{V_0}(k)$ is given in the third column. As mentioned before all spectral power estimation methods have an under limit on the variance that is intrinsically present. This limit depends on the window. On top of that there is an additional term

Table 5: Leakage + interpolation error for a period of length N and an overlap r

window	bias	Normalized variance $M\sigma^2_{\hat{S}_{V_0}}(k)/S_{V_0}(k)$
Rect	$O(N^{-1})$	$1/3 + O((1-r)^2)$
Half-sine	$O(N^{-2})$	$0.3 + O((1-r)^3)$
Hanning	$O(N^{-4})$	$1/4 + O((1-r)^4)$

that depends on the overlap and decreases monotonously as a function of the overlap. That is where the additional gain is made. Extensive simulations show that the mean square error ($\text{bias}^2 + \text{variance}^2$) is a monotonously decreasing function of the overlap r, which indicates that the growth of the bias errors with the overlap r is smaller than the reduction of the variance error.

A final comparison of these results to those obtained with the polynomial method is under study at this moment.

Part III: The Errors-In-Variables setup

12. Set-up

In this section we generalize the results for FRF-measurements in the OE-setup to the EIV-setup which assumes noise on the input and output signal. Moreover we also allow for mutual correlation between the input and the output disturbances. In order to avoid systematic errors (bias) on the FRF measurements it will be necessary to generalize the methods of Section 4 and 5, while the methods for periodic excitations in Section 10 can still be applied without any change. The generalized EIV-measurement setup is given in Figure 4. Observe that this setup also includes measurements under feedback conditions. In that case the output disturbances are correlated with the input signals which also can lead to a bias on the FRF-estimates. This makes also clear that Part III is written under the noise Assumption 4b.

In Section 13 we discuss how to generalize the windowing and polynomial methods using instrumental variable concepts. In Section 14 we comment on the use of periodic signals under these generalized measurement conditions.

13. Instrumental variables method for random excitations

The window methods and the polynomial method for measuring the FRF can be interpreted as least-squares estimates that are linear-in-the-parameters, symbolically written as $Y = K(u)\theta$. Because the measured input signal u is used to construct the observation matrix K, the least squares solution $\hat{\theta} = (K^H K)^{-1} K^H Y$ will be biased by the quadratic noise terms that are formed in the $K^H K$ product. These errors can be reduced by using nonlinear averaging methods [29] if the noise on u, y is mutually independent. Here we focus on methods that eliminate the bias by estimating the plant FRF as the ratio of two other asymptotically unbiased FRF estimates. The input/output noise is allowed (can be mutually dependent) at the cost of having access to the exactly known reference signal $r(t)$ (see Fig. 4):

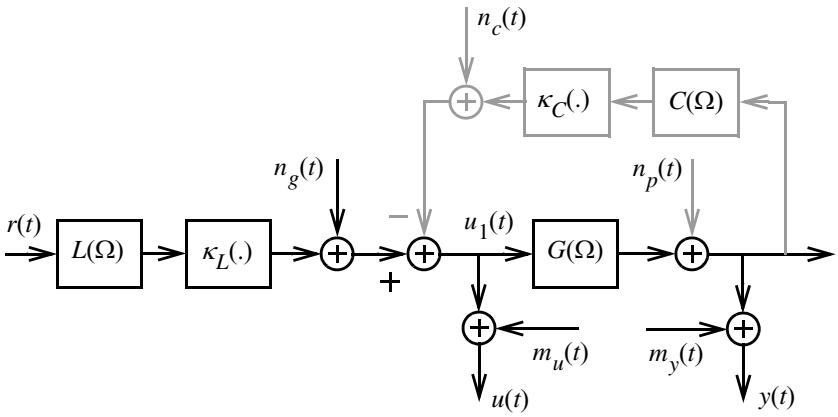

Fig. 4: General errors-in-variables set-up. The reference signal $r(t)$ is applied to the system G. The signals u, y are measured. The system can be captured in a feedback loop. The systems κ_L, κ_C stand for possible nonlinear distortions of the actuator and the controller. n_g, n_C, n_p, m_u, m_y stand for the disturbing noise sources (generator-, controller-, process-, and measurement noise).

$$\hat{G}_{\mathrm{IV}}(\Omega_k) = \frac{\hat{G}_{yr}(\Omega_k)}{\hat{G}_{ur}(\Omega_k)}, \tag{30}$$

with for example $\hat{G}_{ur}$ the FRF from the best linear relation (in least square sense) from $r \to u$. Because the reference signal r is assumed to be exactly known, both intermediate transfer functions estimates $\hat{G}_{yr}, \hat{G}_{ur}$ are asymptotically unbiased using the methods from Part II under the corresponding excitation assumption. Also the error analysis of Part II applies here. With a nonlinear controller or actuator, a part of the information in r will be lost in the linear approximation that is made, resulting in an increased variance on the estimated FRF. The method that is based on periodic excitations does not suffer from this disadvantage. For these methods n_g, n_c are not considered as a part of the excitation signal $u_1(t)$, their contribution to the estimate is completely eliminated.

14. Periodic excitations

Just as for the OE setup, it is possible to calculate the sample means $\hat{U}(k), \hat{Y}(k)$ from which it a direct estimate of the FRF is made using (27). This estimate will be consistent for $M \to \infty$. Of course it is also possible to estimate at the same time the sample (co-variances):

$$\begin{aligned}
&\hat{\sigma}^2_U(k) = \frac{1}{M-1}\sum_{l=1}^{M} \left|U^{[l]}(k) - \hat{U}(k)\right|^2, \hat{\sigma}^2_Y(k) = \frac{1}{M-1}\sum_{l=1}^{M} \left|Y^{[l]}(k) - \hat{Y}(k)\right|^2 \\
&\hat{\sigma}^2_{YU}(k) = \frac{1}{M-1}\sum_{l=1}^{M} (Y^{[l]}(k) - \hat{Y}(k))\overline{(U^{[l]}(k) - \hat{U}(k))}
\end{aligned} \tag{31}$$

The variance on the FRF is then estimated as:

$$\sigma^2_{\hat{G}_{\mathrm{per}}}(\Omega_k) \approx \frac{\left|\hat{G}_{\mathrm{per}}(\Omega_k)\right|^2}{M}\left(\hat{\sigma}^2_Y(k) / \left|\hat{Y}(k)\right|^2 + \hat{\sigma}^2_U(k) / \left|\hat{U}(k)\right|^2 - 2\mathrm{Re}\left(\hat{\sigma}^2_{YU}(k) / \left(\hat{Y}(k)\overline{\hat{U}(k)}\right)\right)\right). \tag{32}$$

The major disadvantage of this method is the requirement to impose periodic signals. Its major advantage is that the user does not need to have access to the reference signal. Moreover, the same solution can be used as well for the EIV as for the OE problems, without requesting any additional information from the user. This makes the method robust and user friendly. Similar to the instrumental variables method, it can also be observed that also in

the periodic approach the generator and controller noise, which are not periodic, will not increase the variance of the estimates due to the presence of the covariance $\hat{\sigma}^2_{\hat{Y}U}$ in (32).

15. Experimental illustration

In this section, some of the previous results are illustrated on a vibrating steel beam. This system has very low damping and was selected to create long transient effects, and hence important leakage errors to get an extreme visualisation of the messages of this paper. The beam is excited in its transverse direction by a mini-shaker (B&K 4810). The force (input) and the acceleration (output) are measured using an impedance head (B&K 8001). These signals are amplified and buffered before being applied to the acquisition channels (HPE 1430A) of a VXI measurement system. The excitations are generated by an arbitrary waveform generator (HPE 1445A) at a sampling frequency $f_s = 10\text{MHz}/2^9 \approx 19.531\text{kHz}$. The output is amplified before being applied to the mini-shaker. Two experiments are performed: the first one with a periodic excitation, the second one with a discrete interval random binary reference signal [31]. The signals have about the same peak value for the reference signal in the arbitrary waveform generator. For the periodic experiment, a crest factor optimized multisine ($N = 1024$ points per period is used with $F = 307$ harmonically related frequencies $kf_s/N \approx k19.07\text{Hz}$, $k = 1, 2, \ldots, F$.

Periodic processing: From the post-processing it turns out that it takes about 10 to 15 periods before the transient drops to 1% of its initial value in the first period, disappearing in the noise level of the measurements. For that reason only the last 36 periods out of 50 are used for calculating the FRF for the periodic excitation. In order to avoid overloaded figures, we did not add the periodic results to the plots. A close inspection shows that they completely coincided with the local polynomial results for the EIV-setup, which confirms the quality of the measurements. Because the period length is 50 times shorter than the length of the noise sequence, the resolution of the periodic data is also 50 times lower. That makes it very difficult to estimate the peak-value of the resonances from the periodic data.

15.1 Analysis 1: output error versus errors-in-variables setup

Using the available data, it is possible to process the measurements in the OE- as well as in the EIV-setup. The results for the local polynomial method are given in Figure 5, which shows clearly that the EIV-setup gives better result. From the zoom around the 2nd resonance, it can be seen that the OE under-estimates the peak-value and hence over-estimates the damping. Also the standard deviation on the FRF is much higher for the OE. This is due to the fact that at the resonance the system is very flexible, and it becomes almost impossible to inject power into the system at that frequency. This results in a signal-to-noise of less than 1 at that frequency. Hence the OE-methods will be significantly biased at those resonances. This is an important observation, because damping measurements are an important issue in mechanical measurements.

15.2 Analysis 2: comparison of the window and local polynomial method for the EIV-setup

In this analysis we compare the local polynomial method with the classical windowing results using a Hanning window. For the window methods, the noise record was split in 12 sub-blocks in order to be able to average the results and to avoid dips in the averaged input spectra in $\hat{S}_{RR}$. This reduces the resolution with a factor 12 with respect to the polynomial method. From Figure 6 it can also be seen that the peak values are significantly

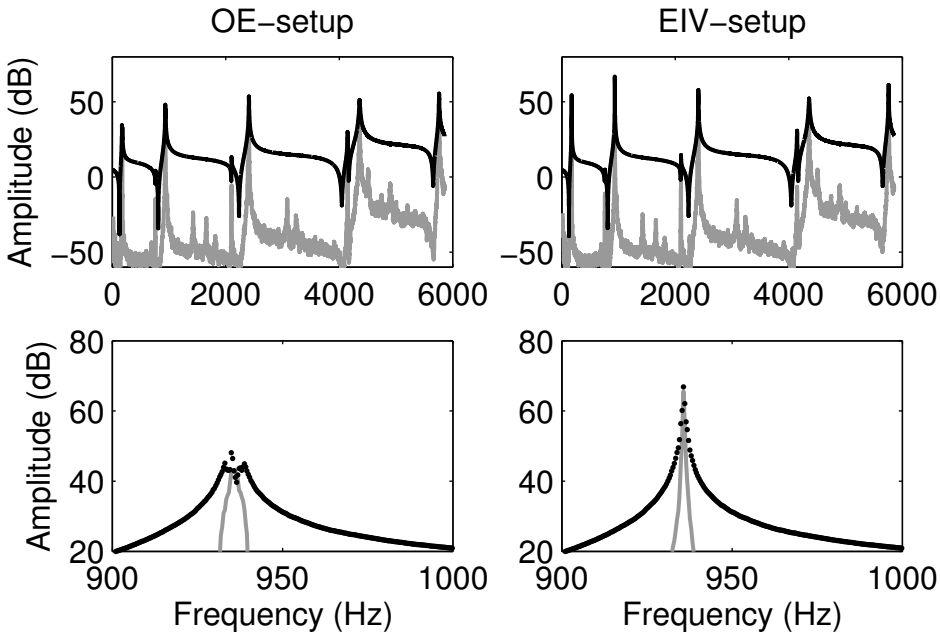

Fig. 5: Comparison of the OE- and the EI-setup for the Local Polynomial method for the EIV-setup. Black lines or black dots: the FRF; gray lines or gray dots: the standard deviation. Top: full view, botton: zoom around the 2nd resonance.

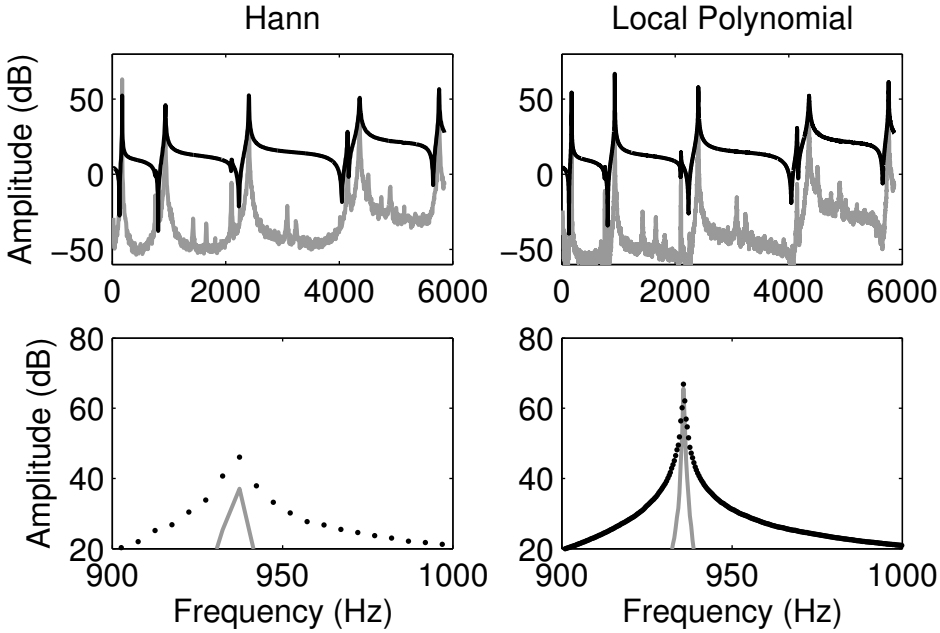

Fig. 6: Comparison of the windowing method (Hanning-window) with the Local Polynomial method for the EIV-setup. Black lines, dots: the FRF; gray lines/dots: the standard deviation. Top: full view, botton: zoom around the 2nd resonance.

underestimated in the window method. This is not only due to reduced resolution but also due to the larger interpolation errors (see Table 2).

16. Conclusion

In this paper we studied a series of classical nonparametric estimation methods for the FRF, the disturbing noise power spectrum, and the spectral analysis of random signals. Starting from a better insight in the smooth behaviour

of leakage errors, a characterization of the leakage and interpolation errors of the classical windowing methods is made. In a next step, improved methods are proposed that reduce significantly these errors. It turns out that the local polynomial method provides high quality estimates for rough excitations that include amongst others random noise signals. As such it combines the best of the random excitation and periodic excitation approach: 1) It keeps and even increases the frequency resolution of the analysis because there is no need to measure multiple periods or split the measurements in a series of sub-records. 2) The method works on random, deterministic, and periodic excitations. For periodic excitations, it is no longer necessary to wait until the transients disappeared, the polynomial method uses all information in the signals, including the transients. This allows the FRF to be measured on the full data record, and make use of the more advanced periodic possibilities on that part of the record where no visible transient is present. 3) The polynomial method is user friendly. It is not necessary to force the user to set some parameters in the method. It is so robust that working with default settings provides excellent results in most cases. In extreme cases, like the mechanical example, it might be necessary to tune the number of frequencies n that is combined.

The major disadvantage is the increased calculation effort, at each frequency a set of equations has to be solved. As such the polynomial method replaces measurement time by increased computation power requirements. While the latter becomes cheaper over time, measurement time remains expensive.

As mentioned before, all these results are already extended to the MIMO case.

From this we can conclude that extremely good nonparametric estimates can be obtained before starting the parametric estimation step in the identification process. This provides the user with very valuable information to judge the complexity of the problem at hand, and to verify the quality of the experimental data in an early phase. It also simplifies popular identification methods like Box-Jenkins because the parametric noise model can be replaced by a nonparametric one so that the model order selection can be restricted to the plant model. Moreover, making use of the frequency domain implementation, it is possible to focus the method on arbitrary user selected frequency bands, without affecting the estimated noise model.

For these reasons, we strongly believe that nonparametric methods will take a more dominant place in the future system identification process.

17. Acknowledgement

This work is sponsored by the Fund for Scientific Research (FWO-Vlaanderen), the Flemish Government (Methusalem 1), and the Belgian Federal Government (IUAP VI/4).

18. References

1. Ljung L. System Identification: Theory for the User (second edition). Prentice Hall, Upper Saddle River, New Jersey 1999.
2. Söderström T and Stoica P. System Identification. Prentice-Hall, Englewood Cliffs 1989.
3. Pintelon R and Schoukens J. System Identification. A Frequency Domain Approach. IEEE-press, Piscataway 2001.
4. Schoukens J, Pintelon R, Dobrowiecki T and Rolain Y. Identification of linear systems with nonlinear distortions. Automatica 2005; 41: 451-504.
5. Bendat JS and Piersol AG. Engineering Applications of Correlations and Spectral Analysis. Wiley, New York 1980.
6. Brillinger DR. Time Series: Data Analysis and Theory. McGraw-Hill, New York 1981.

7. Wellstead PE. Non-parametric methods of system identification. Automatica 1981; 17: 55-69.

8. Rabiner L, Allen J. On the implementation of a short-time spectral analysis method for system identification. IEEE Trans. Acoustics, Speech, and Signal Processing ASSP 1980; 28: 69-78.

9. Douce JL and Balmer L. Transient effects in spectrum estimation. IEE Proc. Pt. D 1985; 132: 25-29.

10. Douce JL and Balmer L. Statistics of frequency-response estimates. IEE Proc. Pt. D 1990; 137: 290-296.

11. Schoukens J, Rolain Y and Pintelon R. Improved frequency response function measurements for random noise excitations, IEEE Trans. Instrum. Meas. 1998; 47: 322-326.

12. Antoni J. Leakage-free identification of FRF's with the discrete time Fourier transform. Journ. of Sound and Vibration 2006; 981-1003.

13. Douce JL. Improving frequency-response estimates by reduction of end effects. IEE Proc.-Control Theory Appl. 2006; 153: 247-250.

14. Harris FJ. On the use of windows for harmonic analysis with discrete Fourier transform. Proceedings of the IEEE 1978; 66: 51-83.

15. Pintelon R, Schoukens J and Vandersteen G. Estimation of nonparametric noise and frequency response funtion models for multivariable linear dynamic systems - Part I: theory, IEEE Trans. Instrum. Meas. 2009; ?: ?-?, (submitted)

16. Pintelon R, Schoukens J and Vandersteen G. Estimation of nonparametric noise models for multivariable linear dynamic systems - Part II: applications and extensions, IEEE Trans. Instrum. Meas. 2009; ?: ?-?, (submitted)

17. Pintelon R, Schoukens J and Vandersteen G. Frequency domain system identification using arbitrary signals, IEEE Trans. Autom. Contr. 1997; AC-42: 1717-1720.

18. Broersen PMT. A comparison of transfer function estimators. IEEE Trans. Instrum. Meas. 1995; 44: 657-661.

19. Antoni J and Schoukens J. A comprehensive study of the bias and variance of frequency-response-function measurements: Optimal window selection and overlapping strategies Automatica 2007;43:1723-1736.

20. Schoukens J, Rolain Y and Pintelon R. Leakage reduction in frequency response function measurements, IEEE Trans. Instrum. Meas. 2006; 55: 2286-2291.

21. Welch P. Use of Fast Fourier Transforms for the estimation of power spectra - a method based on time averaging over short modified periodograms. IEEE Trans. on Audio and Electroacoustics 1967; 15: 70-73.

22. McCormack AS, Flower JO, and Godfrey KR. The suppression of drift and transient effects for frequency-domain identification. IEEE Trans. Instrum. Meas.1994; IM-43: 232-237.

23. Widanage WD, Douce JL, and Godfrey KR. Effects of overlapping and windowing on frequency response function estimates of systems with random inputs. IEEE Trans. Instrum. Meas. 2009; 58: 214-220.

24. Bendat JS. Statistical errors in measurement of coherence functions and input/output quantities, Journ. of Sound and Vibration 1978; 59: 405-421.

25. Schoukens J and Pintelon R. Estimation of nonparametric noise models for linear dynamic systems, IEEE Trans. Instrum. Meas. 2009; 'in print'

26. Guillame P, Schoukens J, Pintelon R, Kollar I. Crest-factor minimization using nonlinear chebysheve-approximation methods. IEEE Trans. Instrum. Meas. 1991; 40: 982-989.

27. Schoukens J, Rolain Y, Simong G, Pintelon R. Fully automated spectral analysis of periodic signals. IEEE Trans. Instrum. Meas. 2003; 52: 1021-1024.

28. Barbé K, Schoukens J, Pintelon R. Non-parametric Power Spectrum Estimation with Circular Overlap. 25th IEEE Instrum. Meas. Technology Conference IMTC, May 12-15, Victoria, Canada. 2008; Proc: 336-341.

29. Guillaume P, Pintelon R, Schoukens J. Nonparametric frequency-response function estimators function estimators based on nonlinear averaging techniques. IEEE Trans. Instrum. Meas. 1992; 41: 739-746.

30. Barbé K, Pintelon R, Vandersteen G. Finite record effects of the Errors-In-Variables estimator for linear dynamic systems. 26th IEEE Instrum. Meas. Technology Conference IMTC, May 5-7, Singapore. 2009.

31. Godfrey KR, editor. Perturbation Signals for System Identification. Prentice-Hall, London 1993.